Heat Transfer and Entropy Generation Minimization in a Lid-Driven Enclosure Filled with Nanofluid

Essma Belahmadi[*] , Rachid Bessaïh

LEAP Laboratory, Department of Mechanical Engineering, Frères Mentouri University-Constantine 1, Constantine 25000, Algeria

Corresponding Author Email: esma.belahmadi@umc.edu.dz

ABSTRACT

This study presents an examination of mixed convection flow within a lid-driven square enclosure containing two cylinders, filled with Al_2O_3-water nanofluid. The finite volume method was employed, utilizing the Ansys-Fluent 14.5 software tool, to resolve the proposed mathematical model. The research was primarily centered on evaluating the impact of varying parameters such as the solid volume fraction (ϕ), Reynolds numbers (Re), and cylinder diameter (D) on heat transfer characteristics and entropy generation (St). As Re was increased, an enhancement in heat transfer was observed, accompanied by a reduction in St and Bejan number (Be). Augmenting ϕ resulted in increased heat transfer and Be, yet decreased St. A surge in D corresponded with elevated St and diminished Be. The investigation indicates that a cylinder diameter of D=0.1H optimizes convective heat exchange and minimizes St, with the average Nusselt number $\overline{Nu}$ consistently decreasing as D escalates. These findings hold substantial potential for the optimization of thermal systems.

1. INTRODUCTION

Fluid flows within confined spaces, coupled with heat transfer, play a pivotal role in realms spanning science and technology, from the cooling of electronic components, heating and air-conditioning systems, to biotechnological processes, among others. The generation of irreversibility, a by-product of thermal resistance and friction in fluid flows, leads to a loss of valuable work during any heat transfer process. Therefore, a primary challenge in thermal engineering involves minimizing a system's entropy generation to maximize available useful work and consequently, enhance the system's energy efficiency. Extensive theoretical, statistical, and empirical studies have probed into these phenomena. Mehryan et al. [1] investigated mixed convection within an oscillating cylinder-induced square enclosure, utilizing Cu-Al_2O_3/water hybrid nanofluid and Al_2O_3. It was found that moving the oscillating cylinder closer to the top and bottom walls enhanced the average Nusselt number $\overline{Nu}$ at low Rayleigh numbers. Moayedi [2] undertook an examination of how rotating cylinder shapes within a vented cavity with inlet and exit ports impacted the flow field, and subsequently, the heat transfer enhancement of laminar Al_2O_3/Cu-water hybrid nanofluid. The Performance Evaluation Index was observed to rise in response to an increase in cylinder rotational velocity, Reynolds number, and nanoparticle volume fraction (ϕ). Continuing this line of study, Alsabery et al. [3] scrutinized transient entropy production and mixed convection, finding that when the cylinder was rotated counter-clockwise with minimum flexible wall deformation, heat transmission and entropy creation reached maximum levels. Similarly, Alsabery et al. [4] explored steady conjugate mixed convection within a double lid-driven square cavity with a solid inner body,

concluding that a large solid body enhanced heat transmission at high Reynolds and Richardson numbers. In a series of investigations, Moayedi [5] calculated rotating cylinders within cavities of various openings in Cu-water nanofluid, demonstrating that the average Nusselt number and Performance Evaluation Criterion (PEC) increased along with nanofluid volume fraction and rotating Reynolds number. Concurrently, Laith et al. [6] analyzed hybrid nanofluid mixed convection within a vented cavity housing an inner adiabatic rotating cylinder. Their numerical studies suggested that heat transmission was enhanced as the cylinder neared the hot wall and rotated counter-clockly. In a differentially heated square enclosure containing a rotating cylinder, Roslan et al. [7] studied convective heat transport. Their findings indicated that the best heat transmission was achieved with high nanoparticle concentration at the enclosure's center, high conductivity, slow positive rotation, and moderate cylinder size. Mirzakhanlari et al. [8] concluded that specific parameter values could maximize the average Nusselt number and decrease the drag coefficient within a square hollow filled with Al_2O_3 nanofluid. Similarly, Alsaberya et al. [9] found that increasing nanoparticle volume fraction enhanced heat transfer within a square enclosure housing a solid circular cylinder. Investigating the effect of nanoparticles, Abu-Nada and Chamkha [10] demonstrated that nanoparticles improved heat transport within an inclined square box filled with water-Al_2O_3 nanofluid. In a 3D hollow filled with nanofluid, Selimefendigil and Oztop [11] observed that the average Nusselt number depended on the rotation direction of two inner adiabatic spinning circular cylinders. Expanding on this, Pandey et al. [12] found that the time and surface-averaged Nusselt number on the cylinder surface increased as the distance between the inner cylinders grew within a four-cylinder enclosure housing

heated cylinders. Costa and Raimundo [13] studied a square enclosure with a spinning cylinder in the center, establishing that the cylinder's thermophysical properties affected heat flow throughout the chamber. Lastly, Alsabery et al. [14] demonstrated that the rotational velocity of a spinning cylinder could influence fluid flow and that the Bejan number reached its maximum for the nearly stationary inner cylinder. Hudhaifa et al. [15] showed that a vented cavity with a heated cylinder between two counter-rotating cylinders achieved the best thermal performance at Re=100.

Given the extensive research in this area, the primary aim of this study is to discern the optimal size of the cylindrical obstacle that could enhance heat transfer while minimizing entropy generation, thereby contributing to the vast literature on this topic.

2. MATHEMATICAL FORMULATION

2.1 Problem description

Figure 1 shows the lid-driven square hollow with two cylinders on the right and left sides of the enclosure. The square cavity's height is H, while the circular cylinders' diameters are 0.1 H, 0.15 H, and 0.2 H. The cavity walls are isothermal, and the top wall can move in the positive x-direction at U. q'' heat flux is assumed for the cylinders. The water-Al_2O_3 nanofluid has uniform, spherical, thermally balanced nanoparticles. Table 1 shows that the thermophysical characteristics of pure water (the base fluid) and nanoparticles stay constant in the Newtonian, incompressible, laminar nanofluid [16].
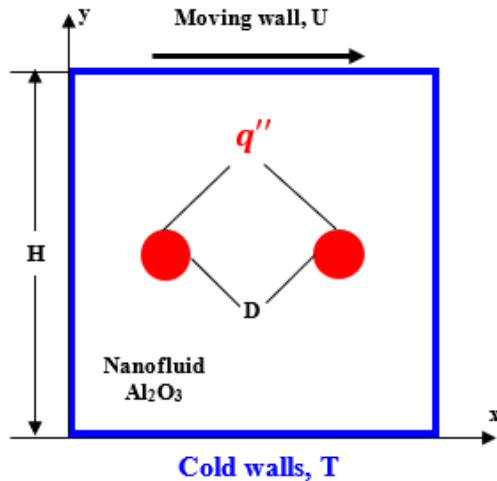

Figure 1. Geometry and boundary condition

Table 1. The thermophysical properties of water and nanoparticles [16]

	ρ (kg.m^{-3})	Cp (J.kg^{-1}.K^{-1})	k (W.m^{-1}.K^{-1})	μ (N.m.s^{-1})
Water	997.1	4179	0.613	1×10^{-3}
Aluminum (Al$_2$O$_3$)	3970	765	40	-

2.2 Governing equations

By considering incompressible laminar flow, the continuity, momentum, and energy equations are expressed:

$$\frac{\partial u}{\partial x} + \frac{\partial v}{\partial y} = 0 \tag{1}$$

$$u\frac{\partial u}{\partial x} + v\frac{\partial u}{\partial y} = \frac{1}{\rho_{nf}}\left[-\frac{\partial p}{\partial x} + \mu_{nf}\left(\frac{\partial^2 u}{\partial x^2} + \frac{\partial^2 u}{\partial y^2}\right)\right] \tag{2}$$

$$u\frac{\partial v}{\partial x} + v\frac{\partial v}{\partial y} = \frac{1}{\rho_{nf}}\left[-\frac{\partial p}{\partial y} + \mu_{nf}\left(\frac{\partial^2 v}{\partial x^2} + \frac{\partial^2 v}{\partial y^2}\right)\right] \tag{3}$$

$$u\frac{\partial T}{\partial x} + v\frac{\partial T}{\partial y} = \alpha_{nf}\left(\frac{\partial^2 T}{\partial x^2} + \frac{\partial^2 T}{\partial y^2}\right) \tag{4}$$

The properties of the nanofluid are described as [17, 18]:

$$\rho_{nf} = (1-\phi)\rho_f + \phi\rho_s \tag{5}$$

$$(\rho c_p)_{nf} = (1-\phi)(\rho c_p)_f + \phi(\rho c_p)_s \tag{6}$$

$$(\rho\beta)_{nf} = (1-\phi)(\rho\beta)_f + \phi(\rho\beta)_s \tag{7}$$

$$\alpha_{nf} = k_{nf}/(\rho c_p)_{nf} \tag{8}$$

$$\mu_{nf} = \mu_f(1-\phi)^{-2.5} \tag{9}$$

$$k_{nf} = k_f\left[\frac{(k_s + 2k_f) - 2\phi(k_f - k_s)}{(k_s + 2k_f) + \phi(k_f - k_s)}\right] \tag{10}$$

2.3 Boundary conditions

The dimensional boundary conditions that solve Eqs. (1) to (5) are illustrated in Table 2.

Table 2. Boundary conditions

Walls	Hydrodynamic Condition	Thermal Condition
Horizontal top wall	u=1, v=0	T=10°C
Other walls	u=0, v=0	T=10°C
Cylinders	u=0, v=0	$q'' = 100\ (W/mm^2)$

2.4 Nusselt number and entropy generation

The following formula is used to calculate the local Nusselt number:

$$Nu = \frac{hD}{k_{nf}} \tag{11}$$

The mean Nusselt number is estimated by the following formulation:

$$\overline{Nu} = \frac{1}{2\pi}\int_0^{2\pi} Nu(\theta)d\theta \tag{12}$$

The relation of the total entropy generation:

$$S_t = \frac{k_{nf}}{T^2}\left[\left(\frac{\partial T}{\partial x}\right)^2 + \left(\frac{\partial T}{\partial y}\right)^2\right]$$
$$+ \frac{\mu_{nf}}{T}\left\{2\left[\left(\frac{\partial u}{\partial x}\right)^2 + \left(\frac{\partial v}{\partial y}\right)^2\right]\right.$$
$$\left. + \left(\frac{\partial u}{\partial x} + \frac{\partial v}{\partial y}\right)^2\right\} \tag{13}$$

3. NUMERICAL METHOD AND CODE VALIDATION

Ansys-Fluent 14.5 software tool was utilized to solve the mathematical model using the finite volume method. A second-order scheme was employed. Convergence in U, V, and T was achieved when the maximum change between two consecutive iterations was less than 10^{-5}.

3.1 Analysis of Grid independence

For D=0.15 H, 0.03, and Re=400, four uniform meshes were chosen to study grid independence. Nu was unchanged by increased nodes (as presented in Table 3). All following numerical simulations used the M3 mesh.

Table 3. Results of grid independence study at D=0.15 H, ϕ=0.03 and Re=400

Grid Name	M1	M2	M3	M4
Number of elements	26000	34000	38000	42000
$\overline{Nu}$	12.39717	12.43281	12.44796	12.45879

Table 4. Compares the mean Nusselt number of a lid-driven inclined square enclosure filled with a nanofluid to that of a standard square enclosure

(Ri=1)		
ϕ	$\overline{Nu}$ [10]	$\overline{Nu}$ [Present study]
0	1.881	1.93
0.02	1.935	1.99
0.05	2.035	2.10
(ϕ=0)		
Ri	$\overline{Nu}$ [10]	$\overline{Nu}$ [Present study]
0.001	7.353	6.503
1	1.881	1.531
10	1.185	1.003

3.2 Code validation

The code was confirmed by the work of Abu-Nada and Chamkha [10] to ensure the accuracy of the current study. This work is focused on the numerical modeling of steady laminar mixed convection flow in a lid-driven inclined square enclosure filled with water-Al_2O_3 nanofluid. The left and right walls of the enclosure are kept insulated while the bottom and top walls are maintained at constant temperatures, with the top surface being the hot wall and moving at a constant speed. The comparison focuses on the Nusselt average number $\overline{Nu}$ (Table 4). According to this table, the current findings are consistent with those of Abu-Nada and Chamkha [10]. The percentage error is 1%.

4. RESULTS AND DISCUSSION

The heat transfer and entropy generation of a lid-driven square enclosure with two cylinders filled with Al_2O_3-water nanofluid under mixed convection were simulated. The simulation covered a wide range of parameters, including (ϕ=0 to 0.05), (Re=100 to 1000), and (D=0.1 H to 0.2 H).

Figure 2 depicts the velocity vectors and isotherms for two Reynolds number values, Re=100 and Re=1000, at D=0.15 H. As expected, a higher Reynolds number means stronger forced convection in the cavity and significant changes in flow and temperature fields. The eddies push the cavity's upper right corner. In addition, a more significant Reynolds number lowers the cavity's maximum temperature.

Figure 3 shows velocity vectors and isotherms for two-cylinder diameters, 0.1 H and 0.2 H, with Re=400 and 0.3. These graphics show that the velocity vectors are similar but flow toward the upper moving wall. The bigger cylinder diameter stagnates fluid flow in the hollow. Increased cylinder diameter moves the isothermal lines toward the cavity's straight wall, reducing heat dissipation and heat exchange area.

Figure 4 shows temperature and velocity profiles in a vertical plane at x=0.8 H from the left vertical wall for various cylinder diameters at Re=400 and ϕ=0.03. Due to natural cavity convection, increasing diameter raises the temperature, as indicated in the figure. D=0.2 H is ideal. However, velocity profiles are unaffected by cylinder diameter. As the cavity diameter rises, fluid flow reduces, reducing absolute velocity magnitude.
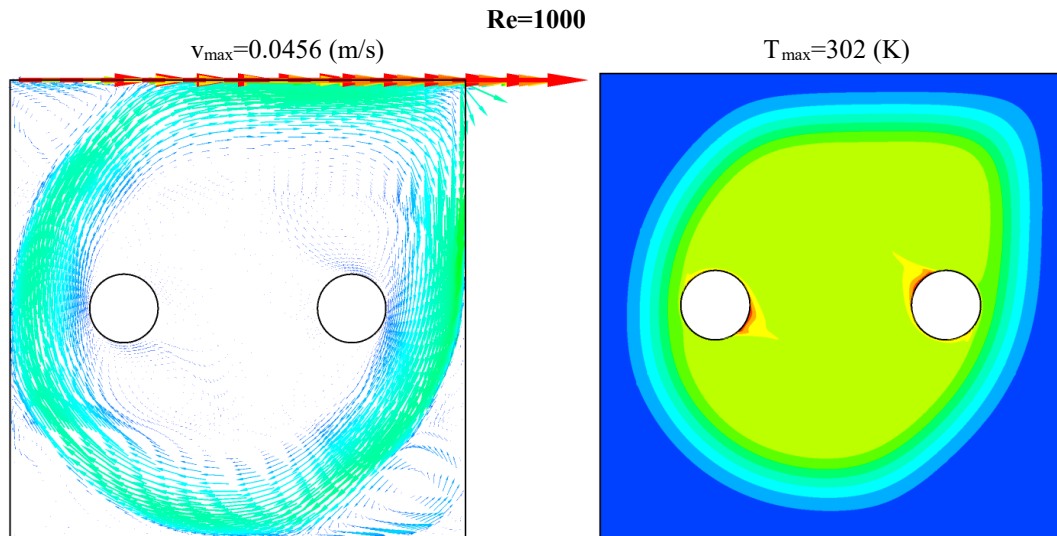
Re=100

v_{max}=0.00456 (m/s) T_{max}=306.5 (K)

Re=1000

v$_{max}$=0.0456 (m/s)   T$_{max}$=302 (K)
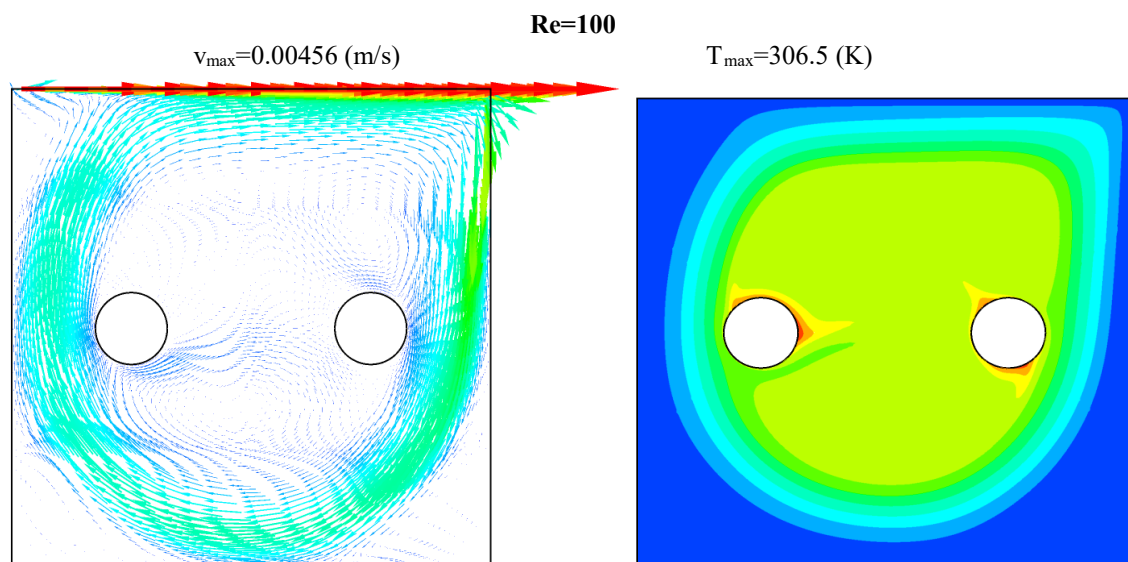
Figure 2. Velocity vectors (left) and isotherms (right) for Re=100 and 1000, at D=0.15 H and ϕ=0.03

D=0.1 H

v$_{max}$=0.01824 (m/s)   T$_{max}$=302.6 (K)

D=0.2 H
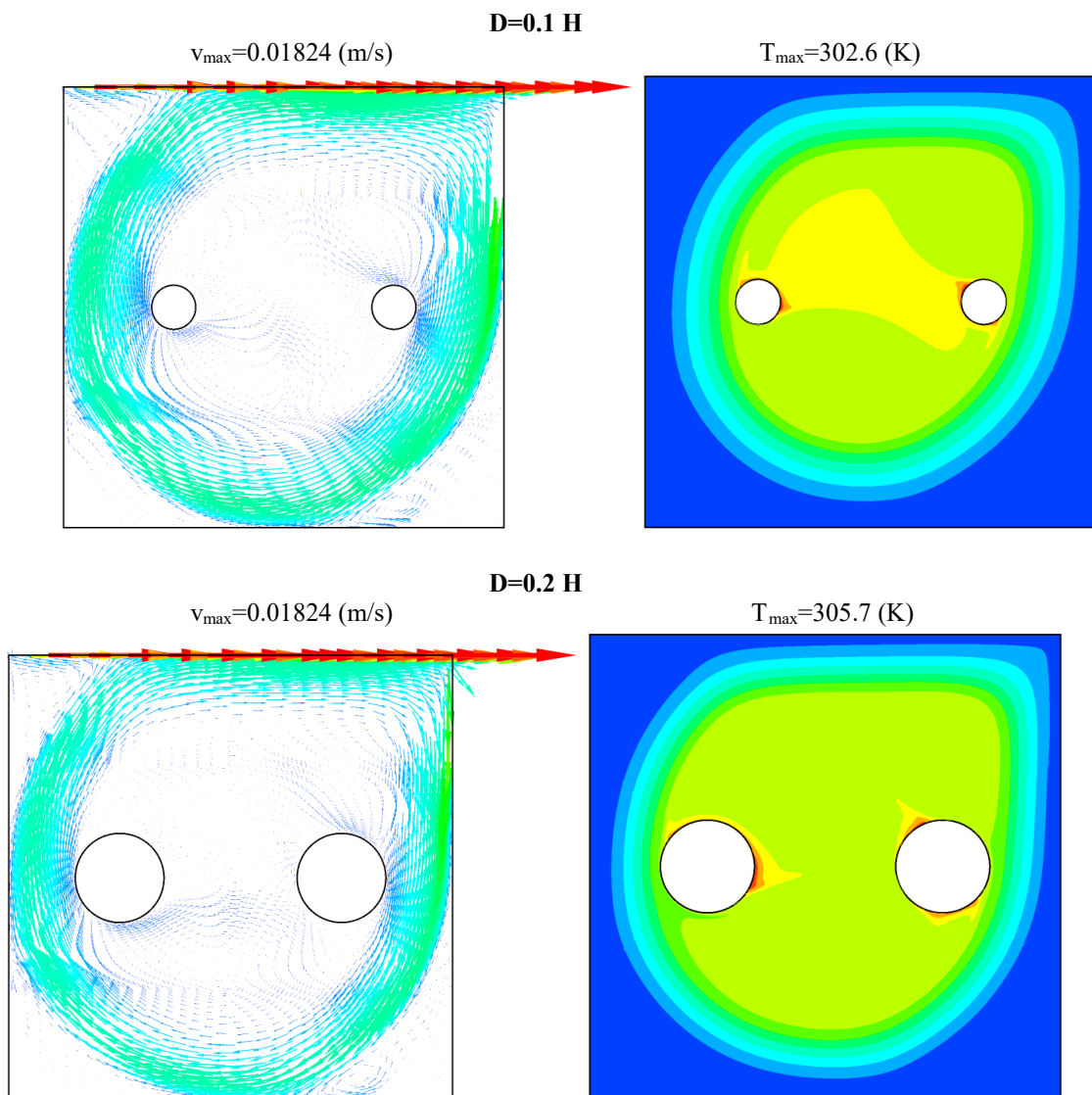
v$_{max}$=0.01824 (m/s)   T$_{max}$=305.7 (K)

Figure 3. Velocity vectors (left) and isotherms (right) for D=0.1 H and D=0.2 H, at Re=400 and ϕ=0.03

Figures 5(a)-(b) show the $\overline{Nu}$ vs. ϕ for different Reynolds numbers (Re) and cylinder diameters (D). Volume fraction raises Nusselt number. Nanoparticles increase base fluid thermal conductivity and heat transfer coefficient. Figure 5(a) shows how Reynolds numbers affect the mean Nusselt number at D=0.15 H. Reynolds number raises mean Nusselt number for all values of. Reduced thermal boundary layer thickness raises the temperature gradient. Inertial effects promote heat

transmission. Figure 5(b) displays the variation of the mean Nusselt number with different cylinder diameters at Re=400. It is observed that the mean Nusselt number decreases with an increase in diameter. Increasing the cylinder diameter limits the fluid flow within the cavity, reducing flow rate and hence heat transfer. There is only a minor difference in the orders of magnitude between D=0.15 H and 0.2 H.

Figures 6(a)-(b) demonstrate overall entropy generation versus nanoparticle volume fraction for varied Re and D. Total entropy generation falls linearly with nanoparticle volume % in all configurations. Increasing base fluid dispersed particles decreases velocity gradients, making velocity gradient the primary factor in entropy formation. Figure 6(a) shows total entropy generation at D=0.15 H for different Reynolds values. Entropy generation reduces with Re. As Re increases, heat transfer entropy production reduces, weakening thermal convection and increasing cavity velocity. Figure 6(b) illustrates total entropy generation for various cylinder diameters at Re=400. Cylinder diameter significantly increases overall entropy generation. The smaller gap between

the cylinders and the chamber improves convection as the cylinder diameter increases.

Figures 7 (a)-(b) show how nanoparticle volume fraction affects Bejan number for various Re and D. Adding nanoparticles to the base fluid raises viscosity, which increases friction irreversibility rate. Figure 7(a) shows the Bejan number variation at D=0.15 H for different Reynolds numbers. Increased Reynolds number decreases Bejan number. Since Bejan number is the ratio of heat transmission to total entropy creation, it accounts for the dominance of heat transfer over friction with lower Reynolds numbers. Reynolds rises, Bejan falls. Figure 7(b) illustrates the Bejan number for different cylinder diameters at Re=400. The Bejan number decreases with cylinder diameter. This indicates that friction dominates heat entropy due to increased fluid-cylinder frictional surface. Be is larger than 0.5 in all configurations, demonstrating thermal irreversibility. When Be>0.5, it indicates that entropy generation is contributed to by temperature gradient. When Be<0.5, it depicts that entropy generation is contributed to by fluid friction.
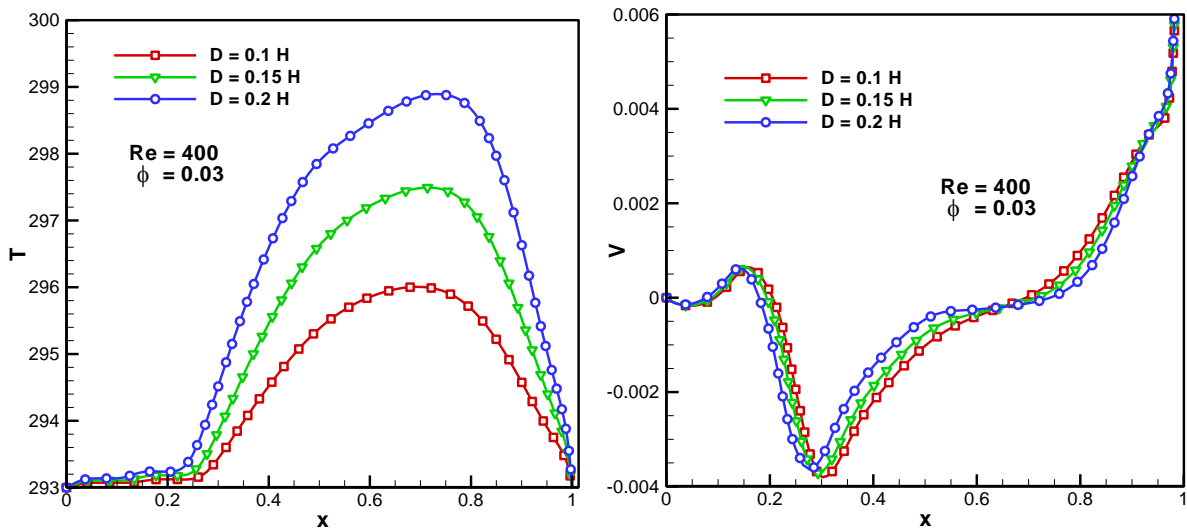

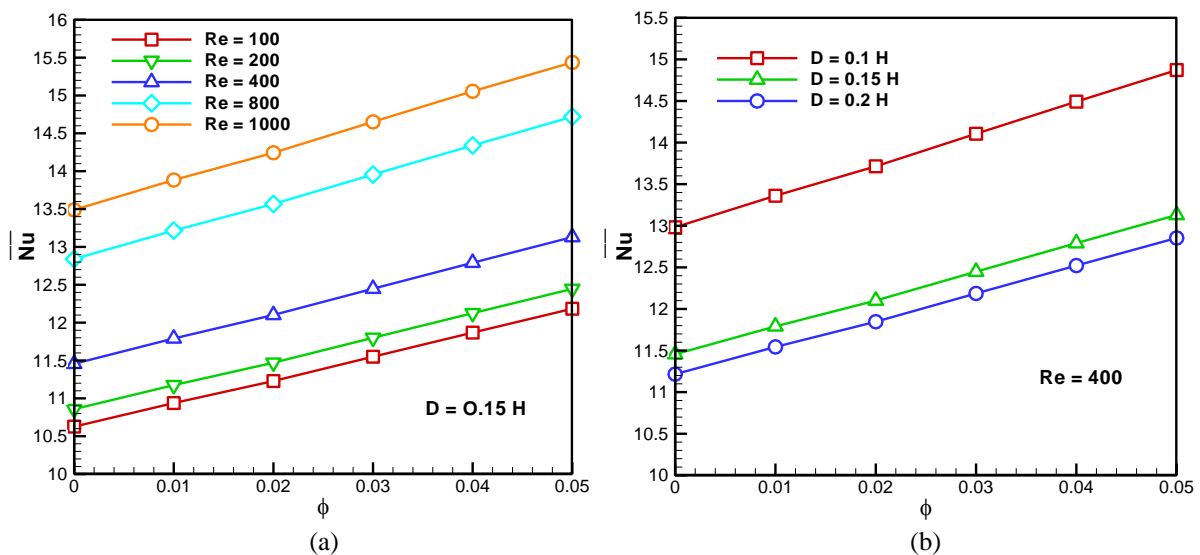**Figure 4.** Velocity and temperature profiles along the vertical plane for various D, at Re=400 and φ=0.03

(a)

(b)

Figure 5. Variation of $\overline{\overline{Nu}}$ with φ for various: (a) Re for D=0.15 H and (b) D for Re=400
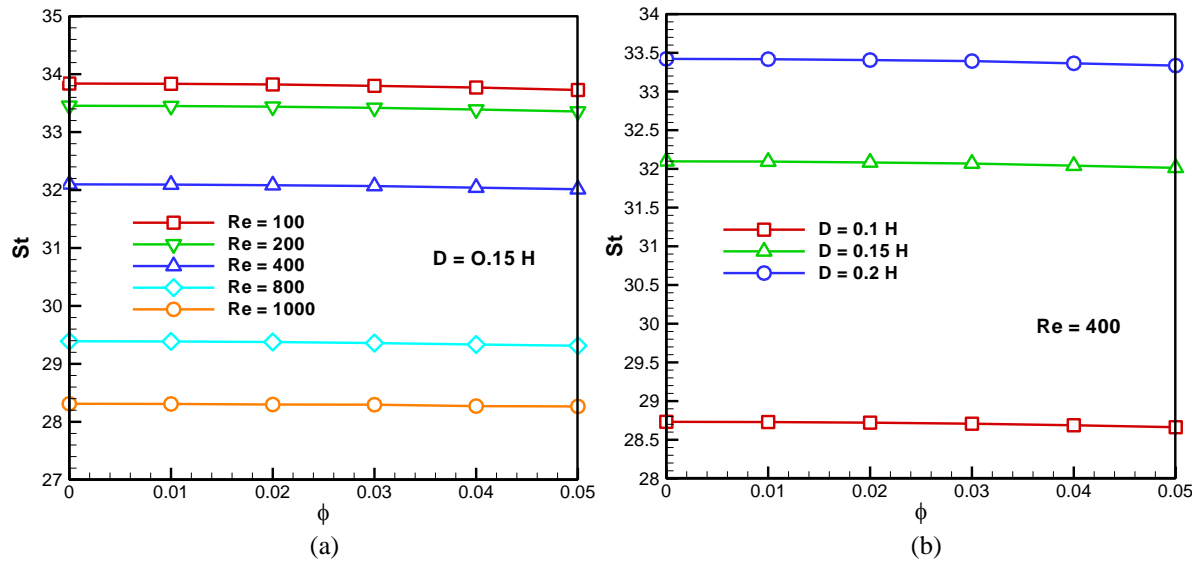
Figure 6. Variation of St with φ for various: (a) Re for D=0.15 H and (b) D for Re=400
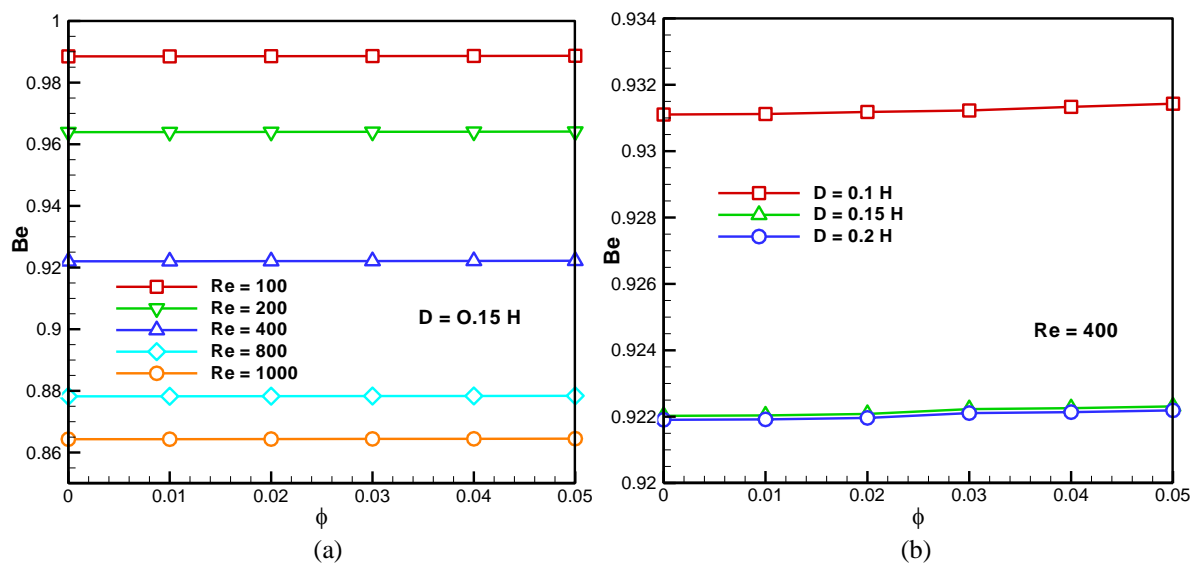

Figure 7. Variation of Be with φ for various: (a) Re for D=0.15 H and (b) D for Re=400

5. CONCLUSIONS

This study explores the mixed convection flow in a lid-driven square enclosure with two cylinders filled with Al_2O_3-water nanofluid, with varying nanoparticle solid volume percentage, Reynolds number, and cylinder diameter. The analysis yields the following conclusions:

- Comparisons with previous results were performed and found to be in excellent agreement.
- Heat transfer increases with an increase in nanoparticle solid volume percentage.
- Entropy generation decreases, and Be increases with nanoparticle solid volume percentage, although both changes are practically constant.
- Reynolds number promotes heat transmission and decreases entropy generation and Bejan number.
- Cylinder diameter increases entropy generation and decreases Bejan number.
- Diameter reduces the average Nusselt number.
- A cylinder diameter of D=0.1 H promotes better

convective heat exchange and minimizes entropy generation.

Nanofluids (NF) are emerging as promising thermofluids for heat transfer applications in various empirical fields and diverse industrial domains, including solar collectors, building ventilation, passive cooling, cooling electronic components, nuclear reactors, food industries, heat exchangers, and more.

REFERENCES

[1] Mehryan, S.A.M., Izadpanahi, E., Ghalambaz, M., Chamkha, A.J. (2019). Mixed convection flow caused by an oscillating cylinder in a square cavity filled with Cu–Al_2O_3/water hybrid nanofluid. Journal of Thermal Analysis and Calorimetry, 137: 965-982. http://doi.org/10.1007/s10973-019-08012-2

[2] Moayedi, H. (2022). Numerical analysis of the effect of configurations of double rotating cylinders on heat Transfer Enhancement Hybrid Nanofluid Flow in a

vented cavity. Journal of Mechanical Engineering Amirkabir, 54: 27-30. https://doi.org/10.22060/mej.2021.19823.7125

[3] Alsabery, A.I., Selimefendigil, F., Hashim, I., Chamkha, A.J., Ghalambaz, M. (2019). Fluid-structure interaction analysis of entropy generation and mixed convection inside a cavity with flexible right wall and heated rotating cylinder. International Journal of Heat and Mass Transfer, 140: 331-345. https://doi.org/10.1016/j.ijheatmasstransfer.2019.06.003

[4] Alsabery, A.I., Ismael, M.A., Chamkha, A.J., Hashim, I. (2018). Mixed convection of Al$_2$O$_3$-water nanofluid in a double lid-driven square cavity with a solid inner insert using Buongiorno's two-phase model. International Journal of Heat and Mass Transfer, 119: 939-961. https://doi.org/10.1016/j.ijheatmasstransfer.2017.11.136

[5] Moayedi, H. (2021). Investigation of heat transfer enhancement of Cu-water nanofluid by different configurations of double rotating cylinders in a vented cavity with different inlet and outlet ports. International Communications in Heat and Mass Transfer, 126: 105432. https://doi.org/10.1016/j.icheatmasstransfer.2021.105432

[6] Laith, M.J., Hudhaifa, H., Cetin, C., Besir, S. (2021). Mixed convection flow of hybrid nanofluid through a vented enclosure with an inner rotating cylinder. International Communications in Heat and Mass Transfer, 121: 105086. https://doi.org/10.1016/j.icheatmasstransfer.2020.105086

[7] Roslan, R., Saleh, H., Hashim, I. (2012). Effect of rotating cylinder on heat transfer in a square enclosure filled with nanofluids. International Journal of Heat and Mass Transfer, 55(23-24): 7247-7256. https://doi.org/10.1016/j.ijheatmasstransfer.2012.07.051

[8] Mirzakhanlari, S., Shirvan, K.M., Mamourian, M., Chamkha, A.J. (2017). Increment of mixed convection heat transfer and decrement of drag coefficient in a lid-driven nanofluid-filled cavity with a conductive rotating circular cylinder at different horizontal locations: A sensitivity analysis. Powder Technology, 305: 495-508. https://doi.org/10.1016/j.powtec.2016.10.029

[9] Alsaberya, A.I., Gedikc, E., Chamkhad, A.J., Hashimb, I. (2019). Effects of two-phase nanofluid model and localized heat source/sink on natural convection in a square cavity with a solid circular cylinder. Computer Methods in Applied Mechanics and Engineering, 346: 952-981. https://doi.org/10.1016/j.cma.2018.09.041

[10] Abu-Nada, E., Chamkha, A.J. (2010). Mixed convection flow in a lid-driven inclined square enclosure filled with a nanofluid. European Journal of Mechanics B/Fluids, 29(6): 472-482. https://doi.org/10.1016/j.euromechflu.2010.06.008

[11] Selimefendigil, F., Öztop, H.F. (2018). Mixed convection of nanofluids in a three dimensional cavity with two adiabatic inner rotating cylinders. International Journal of Heat and Mass Transfer, 117: 331-343. https://doi.org/10.1016/j.ijheatmasstransfer.2017.09.116

[12] Pandey, S., Jakkareddy, P.S., Seo, M.H., Ha, M.Y. (2022). Direct numerical simulation of natural convection between an enclosure and multiple circular cylinders: An influence of horizontal arrangement of

cylinders. Case Studies in Thermal Engineering, 36: 102205. https://doi.org/10.1016/j.csite.2022.102205

[13] Costa, V.A.F., Raimundo, A.M. (2010). Steady mixed convection in a differentially heated square enclosure with an active rotating circular cylinder. International Journal of Heat and Mass Transfer, 53(5-6): 1208-1219. https://doi.org/10.1016/j.ijheatmasstransfer.2009.10.007

[14] Alsabery, A.I., Tayebi, T., Roslan, R., Chamkha, A.J., Hashim, I. (2020). Entropy generation and mixed convection flow inside a wavy-walled enclosure containing a rotating solid cylinder and a heat source. Entropy, 22(6): 606. https://doi.org/10.3390/e22060606

[15] Hudhaifa, H., Cetin, C., Laith, M.J., Besir, S. (2021). Hydrothermal index and entropy generation of a heated cylinder placed between two oppositely rotating cylinders in a vented cavity. International Journal of Mechanical Sciences, 201: 106465. https://doi.org/10.1016/j.ijmecsci.2021.106465

[16] Abu-Nada, E., Chamkha, A.J. (2008). Mixed convection flow in a lid-driven inclined square enclosure filled with a nanodfluid. Enropean Journal of Mechanics B/Fluids, 29(6): 472-482. https://doi.org/10.1016/j.euromechflu.2010.06.008

[17] Brinkman, H.C. (1952). The viscosity of concentrated suspensions and solutions. The Journal of Chemical Physics, 20: 571-581. https://doi.org/10.1063/1.1700493

[18] Maxwell, J.C. (1873). A Treatise on Electricity and Magnetism, Vol. II. Oxford University, Cambridge, UK, 54. http://doi.org/10.1017/CBO9780511709340

NOMENCLATURE

Be	Bejan number
Cp	specific heat, $J.kg^{-1}.K^{-1}$
D	diameter of the cylinder, m
g	gravitational acceleration, $m.s^{-2}$
H	length of square enclosure, m
k	thermal conductivity, $W.m^{-1}.K^{-1}$
Nu	local Nusselt number
$\overline{Nu}$	average Nusselt number
p	fluid pressure, Pa
q''	heat flux, $W.m^{-2}$
Re	Reynolds number
St	dimensional total entropy generation, $J.kg^{-1}.K^{-1}$
T	temperature, K
u, v	velocity components in x, y directions, $m.s^{-1}$
x, y	cartesian coordinates, m

Greek symbols

α	thermal diffusivity of the fluid, $m^2.s^{-1}$
ϕ	solid volume fraction
μ	dynamic viscosity, $kg.m^{-1}.s^{-1}$
ρ	density, $kg.m^{-3}$

Subscripts

c	cold
f	fluid (pure water)
nf	nanofluid
p	nanoparticle